Design of Planar Penetrable Metasurfaces on an Irregular Grid Using Point-Dipole Approximation

Do-Hoon Kwon
Department of Electrical and Computer Engineering
University of Massachusetts Amherst, Massachusetts 01003, USA
dhkwon@umass.edu

***Abstract*—A design technique for free-standing planar metasurfaces comprising an array of subwavelength resonant inclusions on an irregular grid is presented. The local E-field is evaluated as a sum of discrete and continuous contributions from neighboring and far-separated elements, respectively. The dimension of each resonator is determined from the polarizability relation. Free from the limitations associated with unit-cell analysis and design under periodic boundary conditions, the new design technique allows use of irregular grids for functional electromagnetic surfaces.**

I. Introduction

Periodic Green's functions and periodic boundary conditions (PBCs) in numerical analysis have enabled development and maturation of functional periodic electromagnetic structures, such as photonic/electromagnetic bandgap materials, metamaterials, and metasurfaces [1]. By relaxing the condition of identical cells, position-dependent wave-matter interaction can by synthesized for a variety of wave transformation applications [2]. While efficient unit-cell analysis enabled by PBCs allows accurate prediction of mutual coupling, it forces the grid for cell placement to be regular and planar.

Depending on the application, a regular grid may not be optimal or even possible, necessitating use of an irregular grid. This is most evident in doubly-curved conformal surfaces. Efforts have been reported to address conformal grid generation [3], element design for curved surfaces [4], as well as irregular patterning and surface impedance retrieval [5]. However, to date, mutual coupling effect between elements on irregular grids has not been properly taken into account in element designs.

In this paper, a design technique for resonant inclusions on a planar irregular grid for functional surfaces is presented. Each resonator is designed from the polarizability definition and the local E-field is computed as a sum of discrete and continuous source contributions. As an example, a fully reflecting surface in free space on an irregular grid is designed and numerically tested.

II. Point-Dipole Analysis and Design

Electrically small resonant inclusions may be approximated as point dipoles. The strength of the induced dipole moment p is related to the exciting local E-field E^{loc} via the electric polarizability α as

$$p = \alpha E^{\text{loc}}, \tag{1}$$

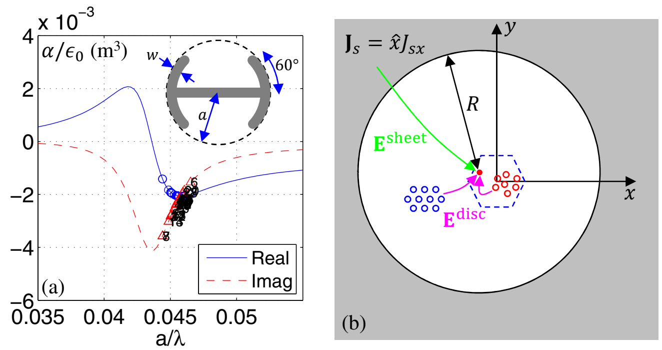

Fig. 1. Individual resonator design approach. (a) The electric polarizability of a planar end-loaded PEC dipole, normalized by the free-space permittivity ϵ_0, with respect to the electrical dimension (λ = free-space wavelength). The strip width is $w = a/5$. (b) Partition of the metasurface plane into discrete and continuous contribution regions and the respective E-field contributions $\mathbf{E}^{\text{disc}}$ and $\mathbf{E}^{\text{sheet}}$ at a dipole location (red dot).

where p and E^{loc} refer to their respective component along the dipole axis. As an example, Fig. 1(a) plots α of a perfect electric conductor (PEC) strip dipole in terms of the dimension a around resonance from FEKO simulation. The dimension of a resonator can be determined once the desired dipole moment and the local E-field are known. For a thin planar metasurface in free space, synthesis of a particular reflection (r) or transmission (t) coefficient under a plane-wave illumination corresponds to realizing a specific average surface current density $\mathbf{J}_s$. If a dipole moment $\mathbf{p}$ is in a cell with an area S, we have $\mathbf{J}_s = j\omega\mathbf{p}/S$ in an $e^{j\omega t}$ time convention.

Consider a metasurface comprising elements on an irregular grid. Since element placement is not periodic, traditional synthesis techniques using unit-cell analysis are not applicable. We resort to (1), where the local E-field is a superposition of external and interaction fields, written as $\mathbf{E}^{\text{loc}} = \mathbf{E}^{\text{ext}} + \mathbf{E}^{\text{int}}$. Furthermore, the interaction field is decomposed as $\mathbf{E}^{\text{int}} = \mathbf{E}^{\text{sheet}} + \mathbf{E}^{\text{disc}}$, as illustrated in Fig. 1(b). At a dipole position under consideration (red dot), fields from all other resonators are split into contributions from neighboring and far-separated elements inside and outside a disc of radius R centered at the dipole, respectively.

This decomposition and analytical evaluation of $\mathbf{E}^{\text{sheet}}$ led to efficient and accurate evaluation of the interaction constant for planar regular arrays [6]. The same strategy can be employed

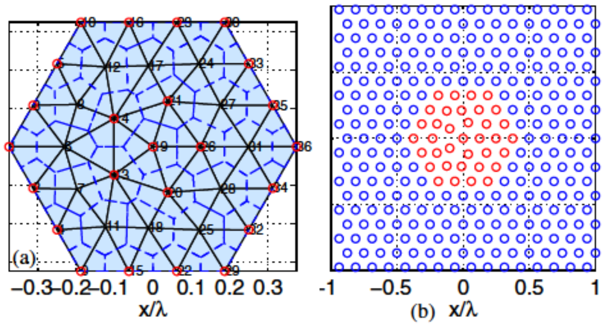

Fig. 2. Design of an example irregular grid. (a) An irregular-grid supercell containing 36 nodes including a pentagonal cell at node 9. Fixed nodes during grid generation are indicated as red circles. (b) Element positions in an infinite planar array. The supercell in (a) (red circles) is surrounded by regular hexagonal grid points extending to infinity.

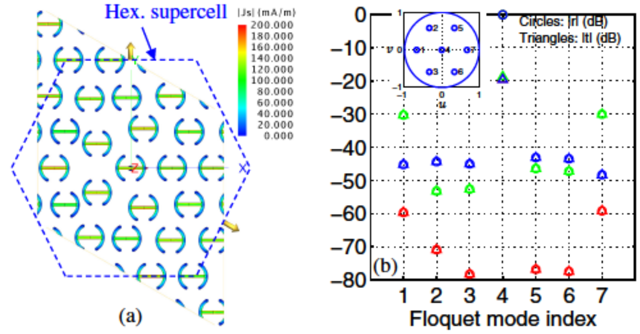

Fig. 3. Simulation of the reflecting metasurface using the supercell method. (a) Magnitude of the induced surface current. (b) Reflection and transmission magnitudes for three cases: the regular-grid supercell (red), the irregular-grid supercell with all-identical unmodified dipole dimension (green), and the irregular-grid supercell with individually tailored dipoles (blue).

to find the location-dependent local E-fields for dipoles on an irregular grid. The sheet contribution from the continuous, homogeneous current $\mathbf{J}_s$ is equal to [6]

$$\mathbf{E}^{\text{sheet}} = -\mathbf{J}_s \frac{\eta}{4}\left(1 - \frac{1}{jkR}\right) e^{\ jkR}, \tag{2}$$

where $k = 2\pi/\lambda$ and $\eta \approx 377\ \Omega$ are the free-space wavenumber and intrinsic impedance, respectively. The E-field from the neighboring elements inside the disc, $\mathbf{E}^{\text{disc}}$, is evaluated as a superposition of individual resonator contributions, assuming that each resonator behaves as a point dipole.

III. Numerical Example

A planar irregular grid together with individual dipole elements are designed and tested. Figure 2(a) shows a regular hexagonal supercell with a side of $3\lambda/8$ that includes a pentagonal cell with a side of $p_0 = \lambda/8$ at the origin. For a given metasurface response, the design objective is to find the dimensions of the 36 dipoles to perform identically as a group of identical dipoles on a regular hexagonal grid. The complete node positions in the xy-plane are shown in Fig. 2(b), which is a union of the irregular-grid supercell (red circles) and a regular hexagonal grid (blue circles).

For a dipole with $a = 0.045$ m, unit-cell FEKO simulation using a hexagonal cell of a side p_0 reveals that the infinite periodic array fully reflects a normally incident plane wave at $f = 790$ MHz. It is now desired that the same full reflection is reproduced using the grid in Fig. 2(b). As a reference, the point-dipole analysis is performed on the periodic hexagonal grid to find the dipole dimension a. It is found that the point-dipole analysis overestimates the dipole dimension by 10.0%.

Proceeding to the grid in Fig. 2(b), $\mathbf{E}^{\text{loc}}$ is calculated at all grid points using $R = 500p_0$ and is observed to vary appreciably with respect to position. The retrieved dipole dimensions are indicated in Fig. 1(a) together with the associated node numbers. After applying a 10% correction to the retrieved dimensions, the irregular-grid supercell is modeled in FEKO and scattering of a normally-incident plane wave with $\mathbf{E}^{\text{ext}} = \hat{x}e^{jkz}$ V/m is simulated under PBCs (i.e., the supercell method). The induced current density shown in Fig. 3(a) exhibits dipole-to-dipole variations, as expected. Fig. 3(b) compares FEKO results for $|r|$, $|t|$ for three configurations, where the inset shows the directions of the seven propagating Floquet modes in $(u, v) = (\sin\theta\cos\phi, \sin\theta\sin\phi)$. When the dipoles are placed on the irregular grid without adjusting their dimensions, significant undesired propagating modes appear. In contrast, individually designed dipoles suppress all propagating higher-order modes to low levels below –40 dB, demonstrating the effectiveness of the point-dipole analysis and design for irregular grids.

IV. Conclusion

A design approach for free-standing planar metasurfaces comprising dipole resonators on an irregular grid has been presented. For synthesizing a particular scattering response, the fundamental polarizability definition is utilized, where the exciting local E-field is efficiently evaluated as a sum of nearby discrete and far-separated continuous source contributions. An example planar metasurface design for full reflection demonstrated the effectiveness of the proposed technique.

ACKNOWLEDGEMENT

This work was supported by National Science Foundation grant ECCS-1930032.

References

[1] S. B. Glybovski, S. A. Tretyakov, P. A. Belov, Y. S. Kivshar, and C. R. Simovski, "Metasurfaces: From microwaves to visible," *Phys. Rep.*, vol. 634, pp. 1–72, 2016.

[2] N. Yu and F. Capasso, "Flat optics with designer metasurfaces," *Nat. Mater.*, vol. 13, pp. 139–150, 2014.

[3] R. C. Rumpf, J. J. Pazos, J. L. Digaum, and S. M. Kuebler, "Spatially variant periodic structures in electromagnetics," *Phil. Trans. R. Soc. A*, vol. 373, pp. 20 140 359/1–22, 2015.

[4] S. M. Kamali, A. Arbabi, E. Arbabi, Y. Horie, and A. Faraon, "Decoupling optical function and geometrical form using conformal flexible dielectric metasurfaces," *Nat. Commun.*, vol. 7, pp. 11 618/1–7, 2016.

[5] J. Lee and D. F. Sievenpiper, "Method for extracting the effective tensor surface impedance function from nonuniform, anisotropic, conductive patterns," *IEEE Trans. Antennas Propag.*, vol. 67, no. 5, pp. 3171–3177, May 2019.

[6] S. Tretyakov, *Analytical Modeling in Applied Electromagnetics*. Norwood, MA: Artech House, 2003.